ACS OMEGA

Open Access

http://pubs.acs.org/journal/acsodf

Article

Multisource Heterogeneous Data Fusion-Based Process Monitoring of the Reheating Furnace in Steel Production

Yunqi Ban, Yanyan Zhang, Xianpeng Wang, Yang Yang,* and Zhenyu Wu

Cite This: *ACS Omega* 2025, 10, 13169−13184

Read Online

ACCESS | Metrics & More | Article Recommendations

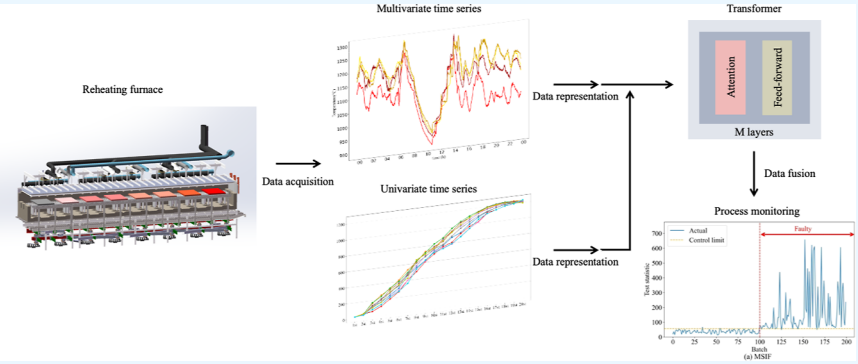

ABSTRACT: The reheating furnace is the key piece of equipment in the hot rolling process of steel production. In order to fully exploit all of the data recorded from the production process representing different information, this paper designs a process monitoring algorithm with multisource information fusion by integrating multiple information to comprehensively monitor the operating state of the reheating furnace. Multisource information fusion combines process variable data of the reheating furnace and heating process data of the slab. To overcome the challenge of fusion of heterogeneous data due to different sampling patterns, univariate time series and multivariate time series data are fused by a transformer. In the fusion scheme, univariate time series data are represented by bidirectional gated recurrent unit for one-dimensional temporal representation, multivariate time series data are represented by temporal convolutional network for two-dimensional temporal representation, and multivariate time series data are represented by eigenvalue decomposition for correlation representation between variables. To evaluate the performance of the proposed method, computational experiments based on actual data are carried out. In univariate and multivariate time series representations, the highest predictions are obtained for bidirectional gated recurrent unit and temporal convolutional network by comparison with different regression algorithms, respectively. By comparing with fusing different fusion objects and different fusion schemes, the proposed algorithm achieves the highest accuracy (91.33%), precision (91.46%), and recall (92.59%), proving the effectiveness of the fusion approach. The process monitoring performance is compared with multivariate statistical process monitoring algorithms, which achieve the highest accuracy (95%), precision (93.45%), and recall (97.08%).

INTRODUCTION

Steel production involves multiple production processes. The raw material, iron ore, starts from the sintering process and goes through the iron making, steel making, hot rolling, and cold rolling processes until the final product is completed. Steel production is energy-extensive and has large equipment in each production process; therefore, it is necessary to detect faults to reduce unnecessary energy waste. A great deal of scholars have tried to design different process monitoring algorithms for content prediction in sintering and strip steel surface defect identification.[1−4]

Hot rolling is a complex production process involving multiple control variables with uncertainty, strong coupling, and multiple operating conditions, and there is strong nonlinearity among the variables.[5] The reheating furnace, which is the key equipment in the hot rolling process, also has similar characteristics. There are usually two types of reheating furnaces, pusher-type and walking beam reheating furnace.[6] The physical illustration of the reheating furnace is shown in Figure 1a. This furnace is a regenerative walking beam type, and the schematic structure is shown in Figure 1b. Reheating furnaces are often divided into various zones, usually into preheating zone, heating zone, soaking zone, etc. Sometimes

Received: November 24, 2024
Revised: March 14, 2025
Accepted: March 18, 2025
Published: March 26, 2025

https://doi.org/10.1021/acsomega.4c10552
ACS Omega 2025, 10, 13169−13184

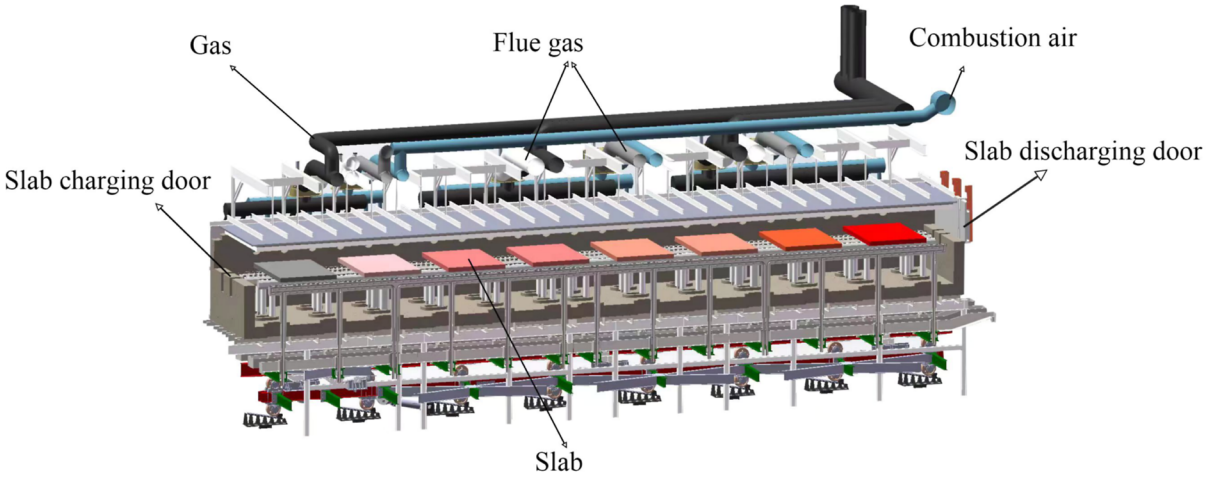

(a) Physical illustration of reheating furnace

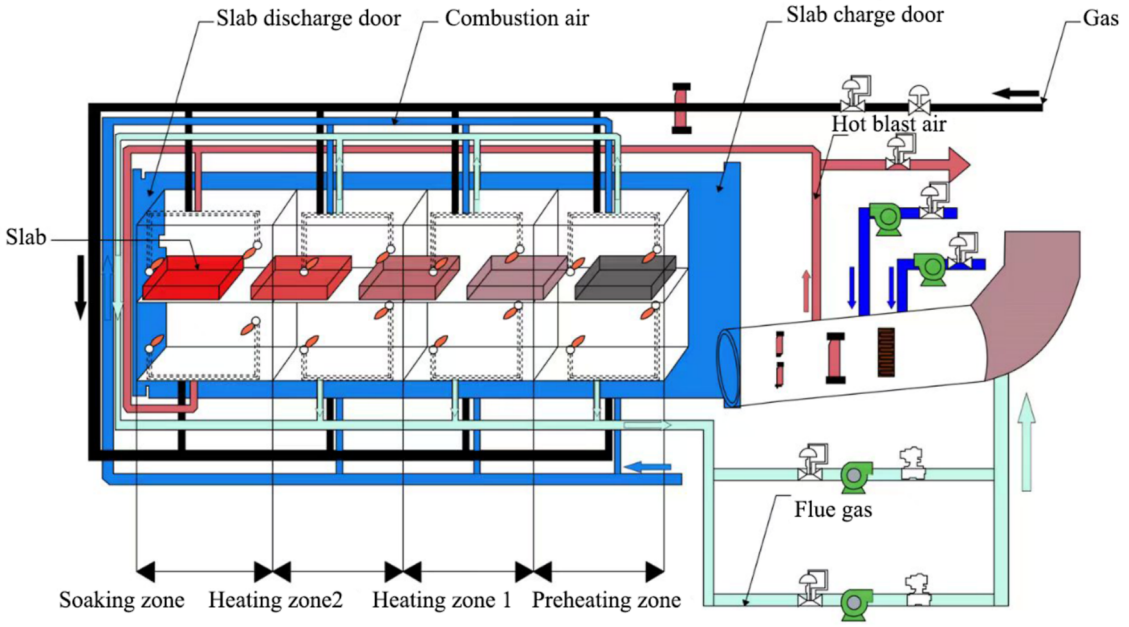

(b) Schematic structure of reheating furnace

Figure 1. Physical view and structural illustration of the walking beam reheating furnace: (a) physical illustration of the reheating furnace and (b) schematic structure of the reheating furnace.

there are more than one heating zone. Depending on the needs of the manufacturing process or following process, each slab is heated for a different period of time, which can be achieved by adjusting the speed of the walking beam. Some slabs may be heated for 2−3 h, while others may be heated for 4−5 h. This results in inconsistent lengths of process variable data of furnace for slabs during the heating process. The heating rate of slabs are realized by adjusting the control variables of the reheating furnace and it is difficult to adjust the gas valve to change the temperature and eventually change the heating process of the slabs inside the furnace in a short time. Further, the temperature variation in the furnace is not synchronized with the heating process of the slab, which causes the temperature variation of the slab later than the temperature variation in the furnace. Every slab is moved by walking beam in the furnace, when it passes through these zones in turn from the entrance to the exit. During the heating process, the slab is heated to the target temperature, which is usually around 1200 °C. Our proposed monitoring scheme depends only on the data recording condition of the reheating furnace and is independent of the type of the reheating furnace, so this monitoring method can be applied to both types of reheating furnaces.

The purpose of the reheating furnace in hot rolling is to heat the slabs to the target temperature and then send them to the subsequent rolling mill for rolling. The heating quality of the slabs will directly affect the quality of the final rolling product. The heating process of a slab usually begins at room temperature, where the steel has a high resistance to deformation. As the temperature increases, the steel begins

https://doi.org/10.1021/acsomega.4c10552
ACS Omega 2025, 10, 13169−13184

to gradually soften, and the resistance of the steel starts to become lower, making it easier to roll. The morphology and distribution of the corresponding microstructure start to change during the temperature increase. The final result is a single-phase austenite with high plasticity and workability. Insufficient heating will lead to insufficient dissolution of carbides and nitrates, which affects the subsequent rolling process with a number of cumulative effects that finally affect the overall steel quality.[7]

Because the temperature inside the furnace is extremely high, and more than 90% of the heat exchange is radiative and a small percentage is convective,[8] there is a strong nonlinearity among the variables of the reheating furnace. The reheating furnace is also characterized by unequal heating times for slabs and a large number of process variables.[9] The slabs usually have different sizes and chemical compositions, which result in complex time-varying states and operating modes in the reheating furnace. Besides the diverse operating conditions, the energy consumption of the reheating furnace is also extremely high[10] and accounts for 70% of the energy consumed in hot rolling and 15% of the energy consumed in steel production,[11] and it is necessary to design process monitoring algorithms for monitoring the operational state of the reheating furnace.

Process monitoring algorithms for reheating furnaces have been proposed in several previous studies.[9,12] Most of the previous process monitoring algorithms for reheating furnaces are usually designed by utilizing single source data. From a chronological perspective, the process variables vary irregularly without a fixed pattern. These difficulties caused some previous works and multivariate statistical methods to not completely monitor the operating status of reheating furnace in a comprehensive way. The inevitable noise also motivates us to fuse multisource data, since anomalies for a given moment have less impact on the overall performance of the algorithm. To overcome these challenges, a process monitoring algorithm fusing multiple sources of data is designed. The judgment of anomaly of the reheating furnace is based not only on the temporal information on the data from multiple sources but also on the correlation that exists among multiple process variables. Moreover, time series data usually have a long time series length, and outliers or missing data at one moment do not affect the performance of our proposed method.

In this paper, a process monitoring algorithm called multisource information fusion (MSIF) is designed with consideration of the characteristics of the reheating furnace. The object is to fuse the process variable data of the reheating furnace and the heating process of the slab, also called heating curve data. Specifically, the temporal representation of heating curve data is performed by bidirectional gated recurrent unit (Bi-GRU), and the process variable data of the reheating furnace are performed by temporal convolutional network (TCN) and eigenvalue decomposition for temporal representation and correlation representation, respectively. The results of the data representation, fusion, and process monitoring are compared with actual production data to illustrate the effectiveness of our proposed method.

RELATED WORK

Process monitoring is crucial to many industrial processes such as the chemical, biological, and food industries. Different process monitoring algorithms are designed to accurately detect the operation of equipment so as to reduce false alarm detection and recognize defects based on the characteristics of industrial equipment. Through the application of process monitoring algorithms, technicians may precisely evaluate the equipment's operational status and make timely adjustments to enhance production process safety and reduce unnecessary energy waste.

With the development of process monitoring, classical principal component analysis (PCA) and its improved versions have been used for process monitoring in a large number of continuous and batch processes. Zhou et al.[13] developed two PCA-based algorithms to monitor the iron-making process and achieve early abnormality detection. Cao et al.[14] proposed a hierarchical hybrid distributed PCA modeling framework to address the problem that a large number of intricately correlated process variables are collected in modern chemical processes. Dong and Qin[15] designed a novel dynamic PCA algorithm to explicitly extract a set of dynamic latent variables in order to capture the most dynamic variations in the data. Kim and Lee[16] presented a multivariate process monitoring method based on probabilistic principal component analysis and explained how the probabilistic method works and was applied to process monitoring through an example. Huang and Yan[17] used kernel least-squares to improve PCA in order to deal with nonlinearity in process monitoring. Wang et al.[18] proposed a multidynamic PCA method based on multiscale neighborhood normalization for detecting faults in a complex batch process with frequent operations. Li et al.[19] demonstrated the effectiveness in batch industrial process monitoring and fault detection by combining time-slice dynamic prediction with enhanced adaptive multiplexed PCA techniques in a new cold rolling mill simulation model.

PCA has been successfully applied for monitoring a multivariate process. However, PCA can only deal with the linear system.[20] Many industrial processes contain both linear and nonlinear components, and kernel principal component analysis (KPCA) is widely used to deal with the nonlinear part of process monitoring. Cho et al.[21] developed a new fault identification method for KPCA. To demonstrate the performance, the proposed method is applied to two simulated processes. Jiang and Yan[22] proposed a parallel PCA-KPCA (P-PCA-KPCA) modeling and monitoring scheme that combines a stochastic algorithm (RA) and a genetic algorithm to efficiently detect faults in processes with linearly and nonlinearly correlated variables. Fezai et al.[23] proposed an online reduced KPCA algorithm for process monitoring to address the issue that KPCA does not perform well in dynamic systems and with large training data sets. Deng et al.[24] proposed a new hybrid linear−nonlinear statistical modeling approach for nonlinear process monitoring by closely integrating linear PCA and nonlinear KPCA using a serial model structure, which is referred to serial PCA. Kano et al.[25] proposed a moving principal component analysis (MPCA) to monitor changes in the direction of each principal component or changes in the subspace spanned by several principal components. Two-dimensional dynamic PCA (2-D-DPCA) is developed for two-dimensional dynamic batch process monitoring.[26] Confronted with the problems of multiphase, asynchronous trajectories and uneven time series batches in time series data, Guo and Zhang[27] proposed sequence moving principal component analysis to deal with the problem of multiphase partition of uneven time batches in time series.

ICA is another dimension reduction tool that can be seen as an extension of PCA. ICA considers higher ordered statistics, which exploit information about cumulants and moments of

https://doi.org/10.1021/acsomega.4c10552
ACS Omega 2025, 10, 13169−13184

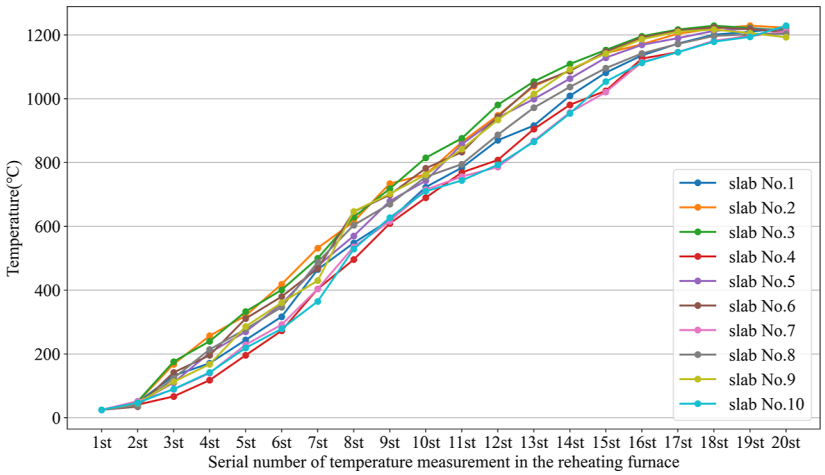

Figure 2. Heating curves for ten batches.

order greater than two. PCA can only impose independence up to second-order statistics information (i.e., covariance) and hence its objective is to decorrelate variables. Oppositely, ICA imposes statistical independence on the individual components by considering higher-order statistics.[28] Thus, ICA can extract latent variables to be non-Gaussian and mutually independent. ICA may reveal more meaningful information in the non-Gaussian process monitoring than PCA.[29] Therefore, for non-Gaussian distributed data, ICA has been applied extensively in monitoring and diagnostic problems.[30] However, traditional ICA lacks probabilistic representation of process uncertainties.Zhu et al.[31] proposed a probabilistic ICA model for non-Gaussian process monitoring and it can achieve more effective industrial process monitoring compared with the deterministic ICA method. Zhou et al.[32] proposed an integrated ICA and PCA method for the case where both Gaussian and non-Gaussian distributions are included in the operating data. This method is applied to the monitoring of blast furnace ironmaking. It was shown that promising results can be achieved in monitoring abnormal furnace conditions in blast furnace ironmaking. Xu et al.[33] proposed a hybrid ICA-PCA method to simultaneously extract the non-Gaussian and Gaussian information on multivariate processes.

In industrial production, multiple sensors record heterogeneous data like sound, temperature, image, and other data. The homogeneous data recorded by only a single type of sensor to determine the operating status of the equipment may result in false decisions and thus affect the reliability. Therefore, process monitoring algorithms should be designed to improve the diagnostic accuracy by fully incorporating data recorded from multiple sensors. Xue et al.[34] proposed a novel framework for motor bearing fault diagnosis from the perspectives of multitransformation domain and multisource data fusion. When confronted with the scarcity of labeled data, Han et al.[35] proposed a novel multisource heterogeneous information fusion network to identify the health status of rotating machinery more comprehensively and robustly under limited data sets. Wang and Wang[36] developed a novel deep learning-based multisource heterogeneous information fusion framework for predicting milling quality. Unstructured data (thermal image) are fused with structured data (time series of multichannel sensors) in this study. MSIF is widely used not only in industry but also in other fields such as biology. Son et al.[37] proposed a fusion transformer for integrating multiple molecular representations with self-supervised learning for molecular property prediction tasks.

Although multivariate statistical process monitoring such as PCA, KPCA, and ICA and improvements based on these methods are widely used in various process monitoring problems, following are the reasons why these multivariate statistical methods are not very suitable for the process monitoring of the reheating furnace.

First, multivariate statistical methods do not need to deal with the case in which the processing time is not the same for each item. For example, the Tennessee-Eastman process has been widely used by the process monitoring community as a source of publicly available data for comparing different process monitoring algorithms. Each batch in the Tennessee-Eastman process runs for identical time. Due to the unequal heating times of slabs, traditional monitoring methods such as PCA, KPCA, ICA, and their improved versions cannot solve our concern problem efficiently. Some related work has been referred to as follows. Yang et al.[12] addressed the problem of unequal times for different slabs with dynamic time warping (DTW), where the process data are equaled in length by transformation, compression and expansion, and subsequently working with multivariate statistical methods. Further, they designed a data preprocessing method of mixed data feature analysis (MDFA) for the operating characteristics of the reheating furnace. The process data of the reheating furnace is handled by MDFA and then the process monitoring is performed by an improved method based on the PCA.[9] Although DTW could give acceptable solutions for data with small differences in length by stretching, compressing, or transforming process variables with inconsistent time lengths into consistent lengths, DTW usually gives unreasonable results in the face of widely varying data.

Second, some multivariate statistical methods also consider unequal time slices. The slab is being heated in the reheating furnace, and a large amount of data is recorded by the various sensors monitoring the diverse procedures and stored in different databases. However, there is no scheme to monitor heterogeneous data together. Traditional monitoring methods such as PCA, KPCA, ICA, and their improved versions cannot monitor multisource heterogeneous data efficiently. Therefore, it is essential to develop a process monitoring algorithm that is suited to the operational and data features of the reheating furnace.

https://doi.org/10.1021/acsomega.4c10552
ACS Omega 2025, 10, 13169−13184

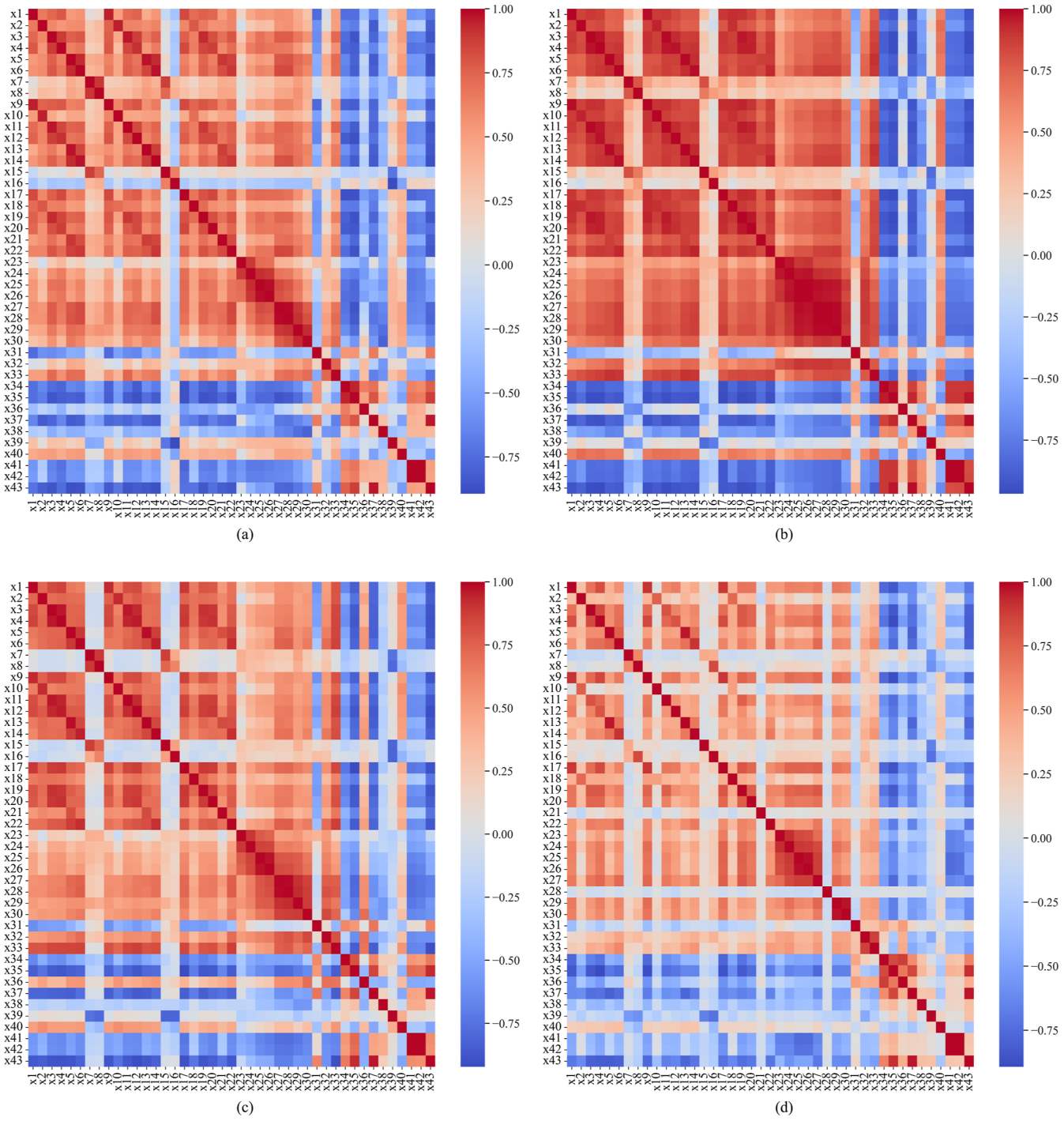

Figure 3. Correlation of the heating furnace process variables: (a−d) results of the correlation analysis of 24 h of operational data.

MODELING OF PROCESS MONITORING FOR THE REHEATING FURNACE

The reheating furnace is a continuous industrial process, like the common chemical processes, having complicated and variable features.[12] In the reheating furnace, the slab is heated to the required temperature. Meanwhile, the quality of the slab is closely related to the running state of the reheating furnace. Process monitoring is mainly used to detect the level of deviation between the operating state and the normal state and to correct the deviation in time to improve the heating quality of the slab and save fuel. Due to the different frequencies and modes of data sampling, two types of data are available during the heating process of the slab. These are univariate time series data indicating the slab heating process by thermocouples installed at equal intervals inside the furnace to measure the surface temperature of the slab, and a multivariate time series is formed by sampling the process variables of the furnace at a fixed time interval. The specific details of MSIF are described in the following content.

Operating Characteristics of the Reheating Furnace. First, we treat each slab as a unit according to the definition in the paper,[9] and the entire heating process for each slab is defined as a batch, which is specified as the slab from entering the furnace to exiting the furnace. Multiple slabs simulta-

https://doi.org/10.1021/acsomega.4c10552
ACS Omega 2025, 10, 13169−13184

neously exist on the walking beam, and the specifications and chemical composition of the slabs also vary from batch to batch. The heating curve data are only related to the number of thermocouples, not the time of sampling. There are 20 thermocouples inside the reheating furnace in this article, so the univariate time series data denoting the heating process for each batch are fixed to 20 dimensions. The heating curve data are shown in Figure 2, which illustrates 10 batches. Batches are at roughly the same temperature at the starting and final temperatures, but the rates of heating are completely different. The device that records the temperature only records a position on the surface of the batch, which does not represent the whole batch at this temperature, but it does give a general description of the process of the temperature rising on the slab.

The data of the process variables of the reheating furnace in operation are calculated as Pearson's correlation coefficients. Red represents a positive correlation, and blue represents a negative correlation, with darker colors representing a higher degree of correlation. The correlation analysis of all the variables with each other is shown in Figure 3 and the equation for calculating the correlation is eq 1. Both x_i and y_i in eq 1 denote each variable in Table 1. Each subplot in Figure 3 indicates the correlation of the process variables running during 1 day. For space constraints, we only show the results for 4 days in the correlation analysis. The specific names of the variables are listed in Table 1. Although not constant, the correlation and degree of correlation between the variables were almost the same over the 4 days. The results of the correlation analysis show that there is a stable correlation relationship between the variables for the operation of the reheating furnace.

$$r = \frac{\sum_{i=1}^{n}(x_i - \bar{x})(y_i - \bar{y})}{\sqrt{\sum_{i=1}^{n}(x_i - \bar{x})^2 \sum_{i=1}^{n}(y_i - \bar{y})^2}} \quad (1)$$

The change in different process variables over the course of a day is presented in Figure 4. The horizontal axis is time and the vertical axis is the value of the process variable. Different types of process variables are illustrated in different rows, where the three rows in Figure 4 represent furnace temperature, gas flow, and pressure, respectively. Moreover, there are multiple heating zones in a reheating furnace, each of those zones will record similar types of process variables. Each graphic in the figure indicates the variations of a single process variable at one location within the reheating furnace. The four columns in first two rows illustrate the top, bottom in the preheating zone and heating zone, respectively. The sensors that record the pressure are not divided according to the heating zones of the reheating furnace. Usually, there are seven pressure sensors in the furnace. In this paper, data from four pressure sensors are selected for presentation, i.e., the pressure of compressed air in the inlet of the reheating furnace (Figure 4i), the pressures of flue gas in the middle of the reheating furnace (shown in Figure 4j,k, which are recorded by two gauges because the flue gases are conveyed by two pipes), and the pressure of hot air formed by heating the air at room temperature in order to aid combustion (shown in Figure 4l). Thus, there are 12 graphics in Figure 4. As can be seen from these figures, the process variables of the reheating furnace operate over a wide range of variations and have complex trends that are difficult to characterize. The simple plan of monitoring the mean values of the process variables and then determining an abnormality if the variation exceeds a certain range is not appropriate.

Table 1. Reheating Furnace Process Variable Description

category of variables	variables	the specific names of the variables
gas flow	×1	gas flow of upper part in preheating zone
gas flow	×2	gas flow of lower part in preheating zone
gas flow	×3	gas flow of upper part in heating zone one
gas flow	×4	gas flow of lower part in heating zone one
gas flow	×5	gas flow of upper part in heating zone two
gas flow	×6	gas flow of lower part in heating zone two
gas flow	×7	gas flow of upper part in soaking zone
gas flow	×8	gas flow of lower part in soaking zone
air flow	×9	air flow of upper part in preheating zone
air flow	×10	air flow of lower part in preheating zone
air flow	×11	air flow of upper part in heating zone one
air flow	×12	air flow of lower part in heating zone one
air flow	×13	air flow of upper part in heating zone two
air flow	×14	air flow of lower part in heating zone two
air flow	×15	air flow of upper part in soaking zone
air flow	×16	air flow of lower part in soaking zone
flue gas flow	×17	flue gas flow of upper part in preheating zone
flue gas flow	×18	flue gas flow of lower part in preheating zone
flue gas flow	×19	flue gas flow of upper part in heating zone one
flue gas flow	×20	flue gas flow of lower part in heating zone one
flue gas flow	×21	flue gas flow of upper part in heating zone two
flue gas flow	×22	flue gas flow of lower part in heating zone two
Temperature	×23	furnace temperature of upper part in preheating zone
Temperature	×24	furnace temperature of lower part in preheating zone
Temperature	×25	furnace temperature of upper part in heating zone one
Temperature	×26	furnace temperature of lower part in heating zone one
Temperature	×27	furnace temperature of upper part in heating zone two
Temperature	×28	furnace temperature of lower part in heating zone two
Temperature	×29	furnace temperature of upper part in soaking zone
Temperature	×30	furnace temperature of lower part in soaking zone
Temperature	×31	temperature of heat recovery
Temperature	×32	temperature of the flue of 1# air preheater
Temperature	×33	temperature of the flue of 2# air preheater
Temperature	×34	temperature at the rear of flue of the gas preheater
Temperature	×35	gas temperature
Temperature	×36	temperature of waste heat boiler evaporator
Pressure	×37	gas pressure of 1# pressure gauge
Pressure	×38	gas pressure of 2# pressure gauge
Pressure	×39	hot air pressure
Pressure	×40	furnace pressure
Pressure	×41	pressure of flue gas of 1# pressure gauge
Pressure	×42	pressure of flue gas of 2# pressure gauge
Pressure	×43	compressed air pressure

The process of heterogeneous data from different sources in the same time period is presented in Figure 5, where the red line is univariate time series data from the heating curve data of a slab. The blue line is the multivariate time series data generated from the process variables of the reheating furnace where only one of the variables is shown for the convenience of presentation. Where Figure 5a indicates that when the flue gas rate is abnormal in a spot within the reheating furnace, specifically over a period of time, there is a continuous value of

https://doi.org/10.1021/acsomega.4c10552
ACS Omega 2025, 10, 13169−13184

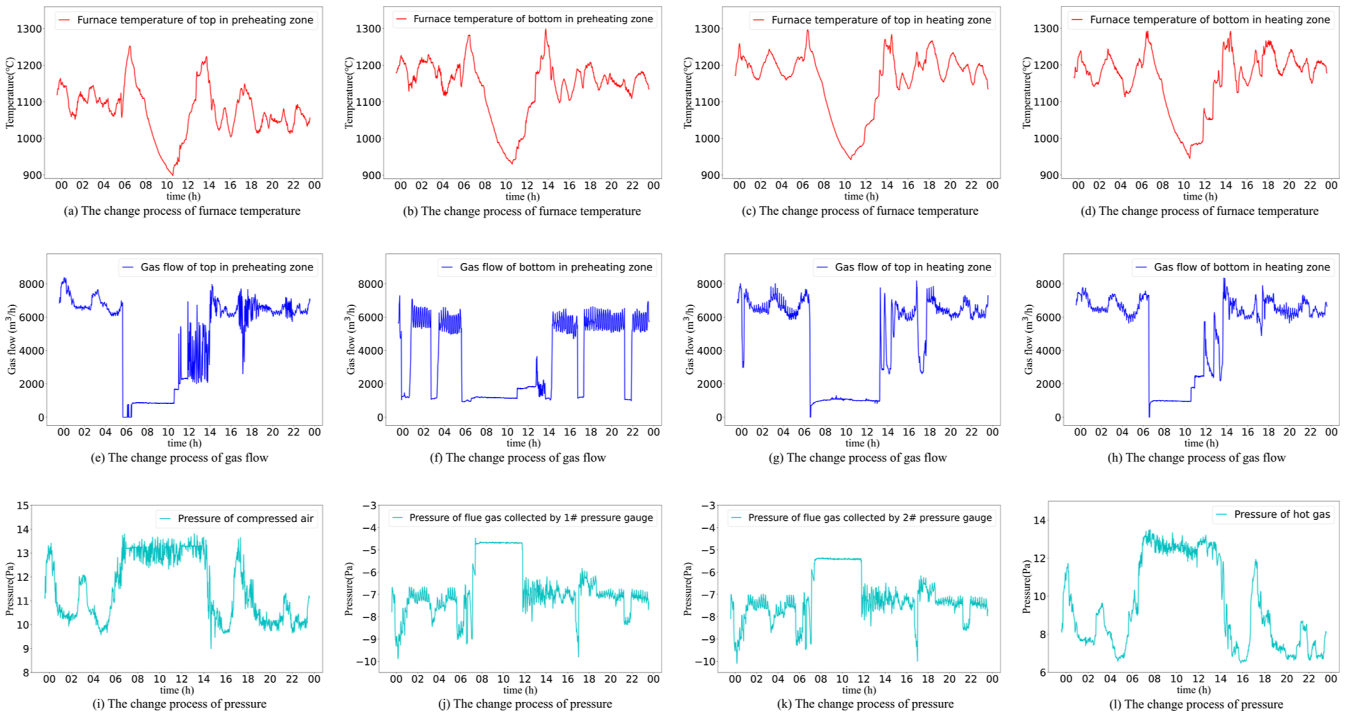

Figure 4. Changing process of process variables in the reheating furnace: (a–d) changing process of furnace temperature; (e–h) changing process of gas flow; and (i–l) changing process of pressure.

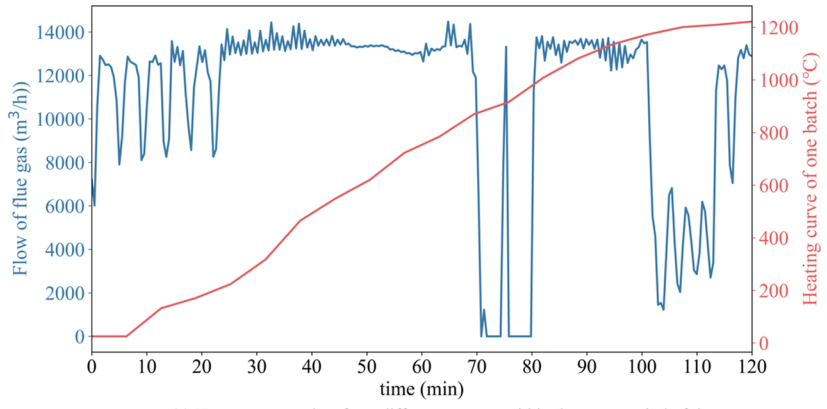

(a) Heterogeneous data from different sources within the same period of time

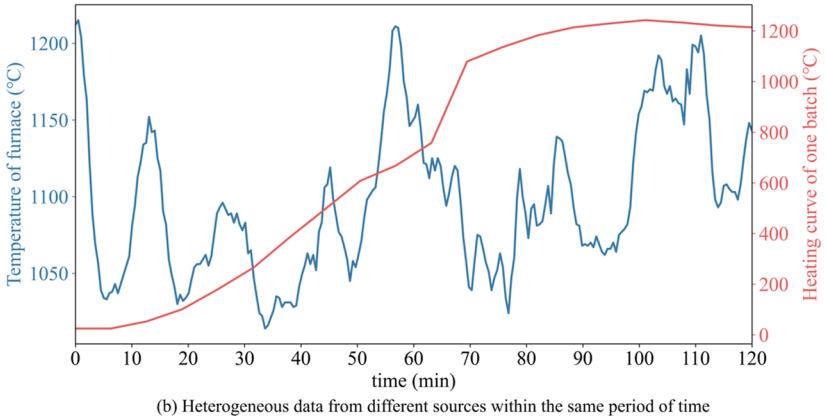

(b) Heterogeneous data from different sources within the same period of time

Figure 5. Process of heterogeneous data from different sources in the same time span.

https://doi.org/10.1021/acsomega.4c10552
ACS Omega 2025, 10, 13169–13184

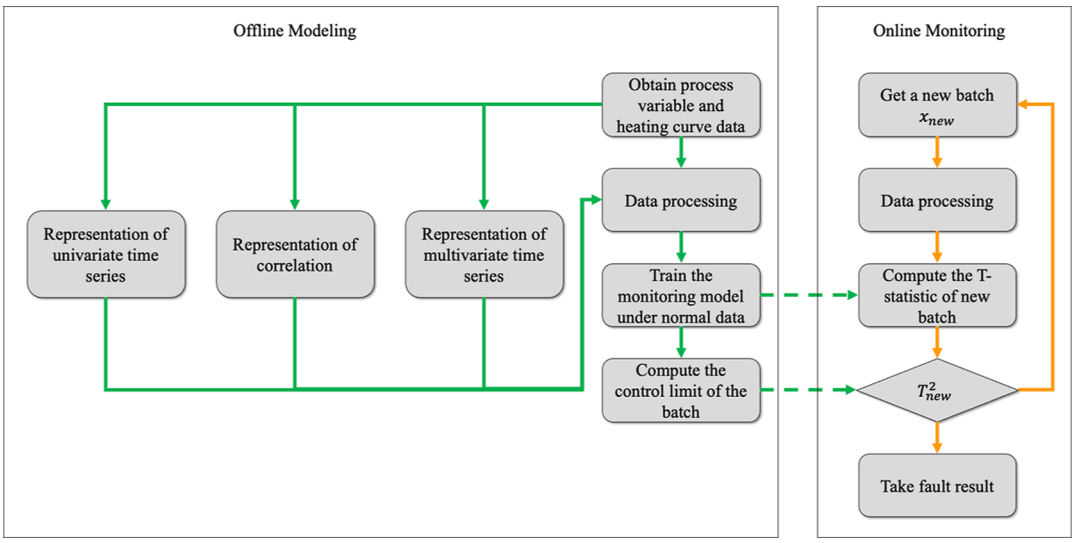

Figure 6. Flowchart of MSIF for the reheating furnace.

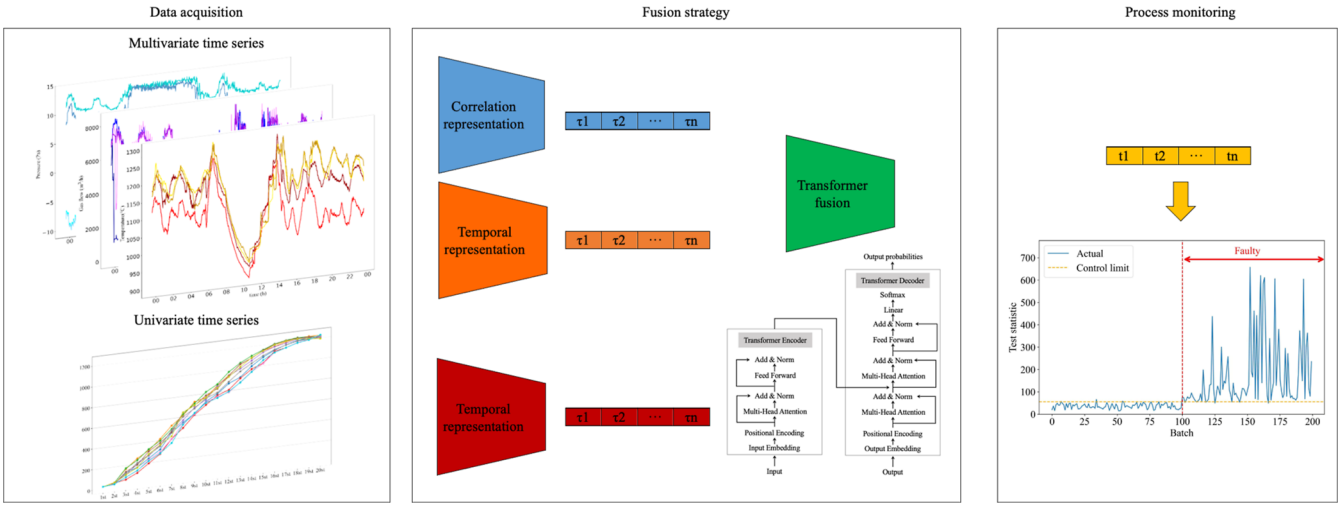

Figure 7. Illustration of the composition of monitoring elements in MSIF.

0 indicating that a region within the reheating furnace is not combusting normally. However, the heating curve data are not abnormal, and are still raising the temperature normally. Figure 5b indicates that there is an abnormal increase in the temperature of the slab, specifically that the heating is reaching a certain temperature and then begins to cool, but the furnace temperature at one spot of the reheating furnace shows that it is still operating normally. The probable causes are all due to the extremely high temperatures inside the furnace, and even though one of the sources has an abnormal, there is a period of time when the anomaly in the other source affects that source. There is a time lag between the effects of each other. Therefore, it is necessary to combine multiple sources of data for process monitoring.

Modeling of Multisource Information Fusion. The implementation flowchart of MSIF is shown in Figure 6. The whole process monitoring algorithm is divided into off-line modeling and online monitoring. Both off-line modeling and online monitoring need data processing. In data preprocessing, the moving average filter is used to smooth the signal from noise fluctuation, and missing as well as outliers data are filled by Lagrange interpolation. In the off-line modeling, normal samples are being used for the modeling. Parameters from the off-line modeling, such as the inverse matrix of covariance and means of the variables for each dimension, are passed into the online monitoring and used to determine the monitoring results of the test sample. Control limit is obtained based on the result obtained from the normal samples and is given to the online monitoring for judgment of the process monitoring result.

In the off-line modeling, Figure 7 shows a schematic diagram of the MSIF. The heating curve data depend only on the number of devices that measure the temperature. So, the heating curve data for each batch is a univariate time series and the time series length is identical for each batch. Due to the production rhythm, not all batches are heated for the same amount of time. Then, for fixed time sampling of process variables, the length is not the same for each batch. So, the process variable data for each batch is a multivariate time series, and the multivariate time series lengths for each batch are not equal.

Based on the two types of data previously described, each batch-monitored object consists of three parts. These are the representation of the temporal information on the univariate

https://doi.org/10.1021/acsomega.4c10552
ACS Omega 2025, 10, 13169−13184

time series data, the representation of the temporal information on the multivariate time series data, and the representation of the correlation of the multivariate time series data. Specifically, the univariate temporal representation is performed by BiGRU. The multivariate temporal representation from all process variables is performed by TCN. Submultivariate time series data are formed by grouping the same category of process variables from all the process variables. Eigenvalue decomposition is performed on each submultivariate time series data, and the eigenvalues obtained represent the correlations of the corresponding categories of process variables. The following sections are to describe the temporal representation of the univariate time series data, temporal representation of multivariate time series data, and correlation of multivariate time series data.

In the face of different data formats, we often make new representations of data that are different from the previous representation in order to facilitate processing. Based on the new representations, we can efficiently perform different analyses, such as forecasting, classification, regression, and anomaly detection.

Representation of Univariate Time Series Data. The Bi-GRU is a time series forecasting method based on the Bi-GRU. It combines a bidirectional model and gating mechanisms to effectively capture temporal relations in time series data.

GRU is a variant of a recurrent neural network with fewer parameters and computational complexity than traditional recurrent neural networks such as long short-term memory (LSTM). It has better performance in dealing with long-term dependencies by incorporating gate units to contain the flow of information.

The Bi-GRU model consists of a two-directional GRU network, with one network processing time series data from front to back and the other processing time series data from back to front. This bidirectional structure captures both past and future information, allowing for a more comprehensive modeling of temporal relationships in time series data. The embedded feature vector by Bi-GRU for univariate time series is shown in eq 2.

$$h_u = \overrightarrow{\mathrm{GRU}}(\mathrm{MLP})(x_s) \oplus \overleftarrow{\mathrm{GRU}}(\mathrm{MLP})(x_u) \tag{2}$$

where x_u denotes the input univariate time series and h_u denotes the representation obtained from the Bi-GRU encoding.

Representation of Multivaritae Time Series Data. Convolutional neural networks (CNNs), which have attracted much attention in the field of deep learning in recent years, have significantly improved the performance of models in feature extraction and pattern recognition tasks by applying convolutional operations to time series data. CNN has already achieved significant results in a number of fields, such as financial forecasting, health monitoring, and industrial equipment fault detection.

The convolutional layer is the most important layer in CNN and is designed to extract features from the input data. The pooling layer is used to subsample the output feature maps of the convolutional layer, thus reducing the size of the feature maps and reducing the number of parameters. The embedded feature vectors of multivariate time series data with CNN is shown in eq 3

$$h_m = \mathrm{POOL}(\mathrm{CONV}(W, X_m) + b) \tag{3}$$

where X_m denotes the input multivariate time series. W and b are the parameters of CNN. h_m denotes the representation obtained from CNN encoding.

Representation of Correlation in the Operation Process. Correlations exist between various process variables during the normal operation of a heating furnace. Submultivariate time series data are combined with the same type of process variables from all process variables in the multivariate time series data. Five submultivariate time series data are formed, which are gas flow, air flow, flue gas flow, temperature, and pressure. The submultivariate time series are eigenvalue decomposed, and the eigenvalues obtained represent the correlation between the process variables. The correlation feature vector is formed by combining all of the eigenvalues obtained above. The correlation feature vector h_c is obtained as in eq 5 where each X_{smi} represents submultivariate time series data grouped according to the category of process variables. The eigenvalue decomposition of singular value decomposition is performed, as shown in eq 4.

$$T = U\Sigma V^T \tag{4}$$

where $U \in R^{N\times d}$, $V \in R^{d\times d}$, $UU^T = I_N$, $V^TV = I_d$, and Σ is the diagonal matrix and the elements are eigenvalues of covariance matrix T and T can be any matrix.

$$h_c = \mathrm{SVD}(X_{sm1}, X_{sm2}, X_{sm3}, X_{sm4}, X_{sm5}) \tag{5}$$

Multisource Heterogeneous Data Fusion in Process Monitoring. The various types of data are turned into corresponding embedded feature vectors by the different methods described previously. However, different feature vectors are independent of each other, and simple concatenation of feature vectors that are heterogeneous to each other may not directly lead to the desired results. Therefore, it is necessary to effectively fuse information from various heterogeneous sources. Transformer is an effective way to efficiently integrate these heterogeneous feature embeddings into a shared subspace. Specifically, the self-attention mechanism within the transformer architecture facilitates the amalgamation of information across multiple representations by modeling dependencies among feature vectors derived from different representations.

The structure of the Transformer is shown in Figure 8. The overall Transformer is mainly divided into two main parts, encoder and decoder. The input sequence is turned into an embedding which is easy to process, then the embedding is passed into the encoder for encoding and mapping into hidden layer features. After encoder combined with the last output is fed into decoder and final probability of the next prediction in the time series is calculated by softmax.

More specifically, the structural input of the transformer starts with positional encoding, which works to mark the temporal or positional relationships between the elements. Encoder consists of multiple identical encoder layers connected in sequence. The encoder layer can be simplified into two parts: a multi-head self-attention and feed-forward network. The former is used to capture the relationship between features, and the latter is used for further encoding learning. Multi-head self-attention is composed of multiple self-attention layers in parallel. In a single self-attention layer, the input is obtained by input embedding and positional encoding with a vector representation of the input data. Next, input data are converted into three transformations to form the three matrices Q, K, and V. The output of a single self-

https://doi.org/10.1021/acsomega.4c10552
ACS Omega 2025, 10, 13169−13184

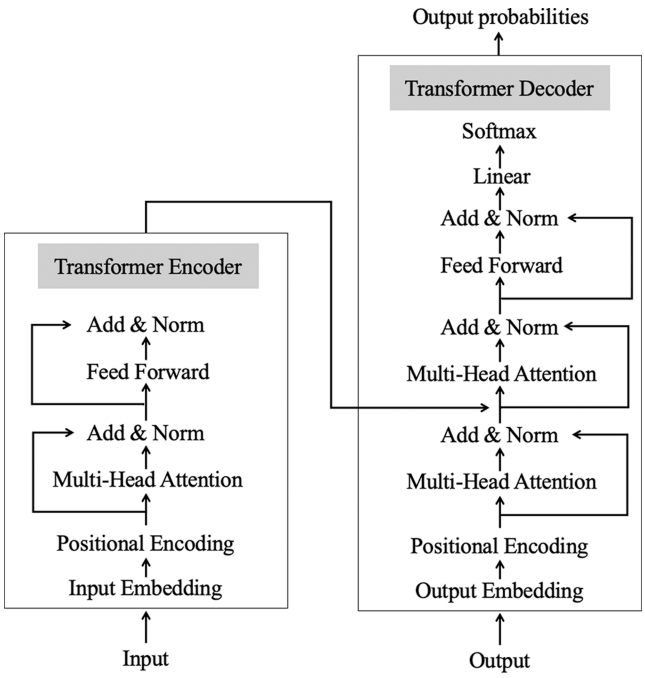

Figure 8. Transformer model architecture.

attention is obtained according to eq 6. Then, the feed-forward network according to eq 7 is joined to form the whole encoder.

$$\text{Attention}(Q, K, V) = \text{softmax}\left(\frac{QK^{\mathrm{T}}}{\sqrt{d_k}}\right)V \tag{6}$$

$$X_{\text{hidden}} = \text{Linear}(\text{ReLU}(\text{Linear}(X_{\text{attention}}))) \tag{7}$$

The decoder consists of mask-multi-head self-attention, multi-head encoder-decoder attention, and feed-forward network as shown in the right part of Figure 8. Mask-multi-head self-attention aims to ignore certain positions and not compute the attentional weights associated with these positions. The K and V matrices in multi-head encoder-decoder attention are taken from the encoder's output, and the Q matrix is the output of mask-output of multi-head self-attention. After all of the layers in decoder are computed, a fully connected layer and softmax layer are added. It is the final result obtained by the transformer.

When all the embedded features are obtained, they pass into the transformer for fusion according to eq 8. Where h_{u} denotes the univariate time series feature representation obtained from Bi-GRU, h_{m} denotes the multivariate time series feature representation obtained from TCN, h_{c} denotes the correlation feature representation obtained from eigenvalue decomposition, and h_{umc} denotes the fusion feature representation of all embedded features combined together.

$$\boldsymbol{z} = \text{transformer}(h_{\text{u}}, h_{\text{m}}, h_{\text{c}}, h_{\text{umc}}) \tag{8}$$

The final output $\mathbf{z} = (z_{\text{u}}, z_{\text{m}}, z_{\text{c}}, z_{\text{umc}})$ is the result of transformation of each of the four inputs by the Transformer. The results are concatenated to obtain the final fusion vector for subsequent computation. The T2 statistic is calculated from the fusion vectors if process monitoring is performed, and the prediction is performed from the fusion vectors if fault detection is performed and then trained by the cross-entropy loss function.

Normal batch samples are trained for the model. During the heating process, many batches are heated at the same time. This will cause the process data of adjacent or close batches to be overlapping parts. In order to make the model have better performance, the process data of the normal training samples do not overlap and ensure a larger interval. The obtained batches are calculated according to eq 9 to calculate the T2 statistic. The formula Λ is the inverse matrix of the covariance composed of normal batches. t_l is the first dimension of the batch minus the mean value of that dimension. The Kernel density estimation method is used to calculate the control limit.

In the online process monitoring, the data acquisition and data preprocessing are kept in the same way as the off-line modeling process. The statistics of each batch are calculated, and the monitoring results are determined. Each new batch sample still uses eq 9 to calculate the T2 statistic. In this equation, the inverse of the covariance matrix and the mean of each dimension are obtained from the training samples. Then, a comparison is made to the control limit. If the calculated T2 statistic is less than the control limit, it is determined as a fault-free batch. If it is greater than the control limit, then it is determined as a faulty batch.

$$T^2 = [t_1, t_2, \cdots t_l]\Lambda^{-1}[t_1, t_2, \cdots t_l]^{\mathrm{T}} \tag{9}$$

EXPERIMENT

The data of the process variable of the reheating furnace are recorded by the sensors of each variable. The sampling frequency of the sensors for each variable is the same, and the data are recorded once every 90 s. The specific number and names of the process variables are shown in Table 1. There are also a number of factors that affect the heating rate such as billet size, steel grade, and the corresponding gas supply. In the batch heating process, no mechanism features are taken into account, and only the heating data are used. The proposed method can be applied to not only different slabs but also bars, pipes, and various other products, just by utilizing the slab for example.

In order to evaluate the superiority of univariate and multivariate time series data representation of model in the test data set, root-mean-square error (RMSE), mean absolute error (MAE), and R^2 (coefficient of determination) are used to measure the degree of fitting. The specific RMSE is defined as eq 10. The calculation formulas of MAE and R^2 are shown in eqs 11 and 12, respectively. In eqs 10−12, n represents the number of data, $\hat{y}_i$ represents the true value of the ith sample, y_i represents the predicted value of the ith sample, and $\hat{y}_{\text{ave}}$ represents the mean value of the true value of the corresponding sample.

$$\text{RMSE} = \sqrt{\sum_{i=1}^{n}\frac{(y_i - \hat{y}_i)^2}{n}} \tag{10}$$

$$\text{MAE} = \frac{1}{n}\sum_{i=1}^{n}|y_i - \hat{y}_i| \tag{11}$$

$$R^2 = 1 - \frac{\sum_{i=1}^{n}(y_i - \hat{y}_i)^2}{\sum_{i=1}^{n}(\hat{y}_i - \hat{y}_{\text{ave}})^2} \tag{12}$$

https://doi.org/10.1021/acsomega.4c10552
ACS Omega 2025, 10, 13169−13184

The heating process of each slab constitutes univariate time series data. The univariate time series has 20 dimensions. The last dimension represents the final temperature to which the slab is eventually heated as a label for the prediction, and the first 19 dimensions are the features of the prediction. 7000 samples are taken as training data, and 1000 samples are taken as test data.

The process data are sampled at 15 s intervals while the batches are heated for 2−5 h with 43 recording positions, which resulted in a large amount of data being recorded. In this way, the process variables of the reheating furnace during the slab heating time formed multivariate time series process data. The process variable data of the reheating furnace are first sliced according to the heating time of each batch. The last moment in the heating time period is used as label value to be predicted. 21,155 instances are treated as training data and 2000 instances are treated as test data.

The effectiveness of the proposed method is validated by comparison with different fusion methods and different fusion objects. Statistical metrics of precision, recall, F1 score, and accuracy are shown in eqs 13−16 to evaluate the performance of the model, respectively. In these equations, TP, FP, TN, and FN denote the number of true positive, false positive, true negative, and false negative samples, respectively. Precision, recall, and accuracy measure the model performance in terms of prediction accuracy of positive samples, coverage ability of true-positive samples, and prediction accuracy of all samples, respectively. The F1 score, which is the reconciled mean of precision and recall, reflects a comprehensive measure of the model performance.

$$\text{Precision} = \frac{\text{TP}}{\text{TP} + \text{FP}} \tag{13}$$

$$\text{Recall} = \frac{\text{TP}}{\text{TP} + \text{FN}} \tag{14}$$

$$\text{F1} - \text{score} = \frac{2 \times \text{precision} \times \text{recall}}{\text{precision} + \text{recall}} \tag{15}$$

$$\text{Accuracy} = \frac{\text{TP} + \text{TN}}{\text{TP} + \text{TN} + \text{FP} + \text{FN}} \tag{16}$$

In the fusion strategy experiment, the training samples are 3000 and the test samples are 600 of which 300 are normal samples and 300 are faulty samples. The parameters of Transformer are 6 of these encoder layers (self-attention layer + feed forward layer), followed by 6 decoder layers, the number of attention heads is 8, and embedding dimension is 64. In the process monitoring experiment, 300 batches are selected as the training sample. The control limit threshold is determined with a confidence level of 0.95. 200 batches are selected as testing samples, among which 100 are normal batches and 100 are faulty batches.

RESULTS AND DISCUSSION

To evaluate the performance of the proposed method, four computational experiments are carried out in this section. First, the results of the univariate and multivariate time series representation by Bi-GRU and TCN are compared with other regression methods. Then, the results of fusion are compared with those of other fusion methods and different fusion objects. Finally the results of process monitoring are compared to other multivariate statistical process monitoring.

Result of Univariate Time Series Representation. In order to validate the superiority of the methodology used to represent univariate time series data, the comparison algorithms are GRU, LSTM,[38] support vector regression (SVR), and K-nearest neighbors (KNN).

The full prediction results are shown in Table 2. As can be seen from the results, Bi-GRU achieves the optimal prediction, specifically 15.241 on the RMSE, 11.626 on the MAE, and 0.489 on R^2. The fitting ability of KNN is the worst among all the compared algorithms. It is also observed that both GRU and LSTM have better prediction results than SVR and KNN from the results. It can be concluded that deep learning-based methods are more advantageous than machine learning-based methods in our problem of univariate time series prediction.

Table 2. Prediction of Slab Heating Temperature by Different Algorithms

	Bi-GRU	GRU	LSTM	SVR	KNN
RMSE	15.241	15.694	16.256	18.075	25.331
MAE	11.626	12.042	12.557	14.232	19.863
R^2	0.489	0.461	0.427	0.292	0.289

The line chart of predicted and actual values on the test data is shown in Figure 9. Figure 9a shows the results for Bi-GRU and Figure 9b shows the results for GRU. It can be seen from the figure that the predicted value of Bi-GRU is much closer to the true value. Bi-GRU consists of two GRUs, one taking the input in a forward direction and the other in a backward direction. Because of this architecture, Bi-GRU has a better predictive performance than GRU. In summary, it is clear from the results that Bi-GRU is suitable for our problem.

Result of Multivariate Time Series Representation. Because of numerous successful applications of CNNs in time series, TCN[39] is applied to model multivariate time series data in this study. To demonstrate the effectiveness of TCN, LSTM, sequence-to-sequence (Seq2Seq), XGboost, and ARIMA which are widely modeled in the field of time series prediction are taken as comparison algorithms. Figure 10 shows the prediction results of TCN on the test data set. Because of the large number of process variables, only the predicted results for three process variables are shown here: the gas flow, blue; the furnace temperature, red; and the pressure in cyan. The horizontal axis is the true value, and the vertical axis is the predicted value. The green dotted line indicates that the predicted and true values are equal. The closer to this line, the better the prediction result. From Figure 10, it can be seen that most of the data points are concentrated around the green line, which proves that TCN has a relatively better prediction result.

Tables 3−5 show the results of different algorithms for gas flow, furnace temperature, and pressure prediction, respectively. TCN leads in all of the predictions from the results. Specifically, in the prediction of gas flow the RMSE is 404.641, MAE is 266.066, and R^2 is 0.787 on the test data. RMSE is 16.223, MAE is 12.514, and R^2 is 0.854 for the furnace temperature prediction on the test data. RMSE is 0.357, MAE is 0.273, and R^2 is 0.802 for the pressure prediction on the test data. LSTM and Seq2Seq are close to each other in terms of prediction ability. XGboost and ARIMA showed worse predictions. It can be seen that deep learning-based models are more advantageous in complex time series prediction problems than statistical-based methods. The prediction results

https://doi.org/10.1021/acsomega.4c10552
ACS Omega 2025, 10, 13169−13184

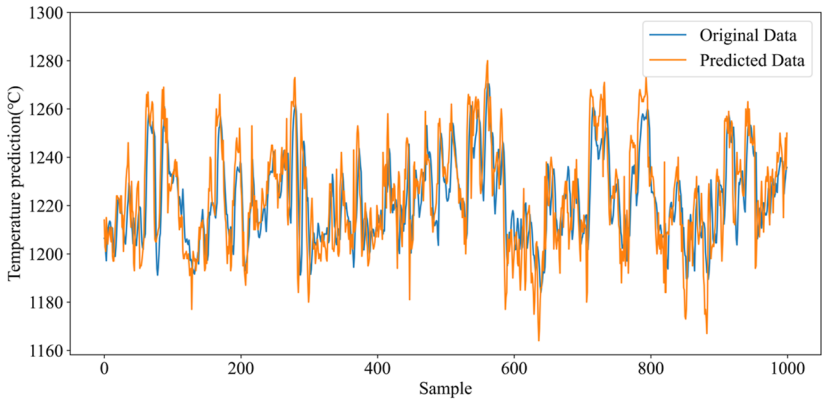

(a) Prediction result of Bi-GRU on univariate time series data

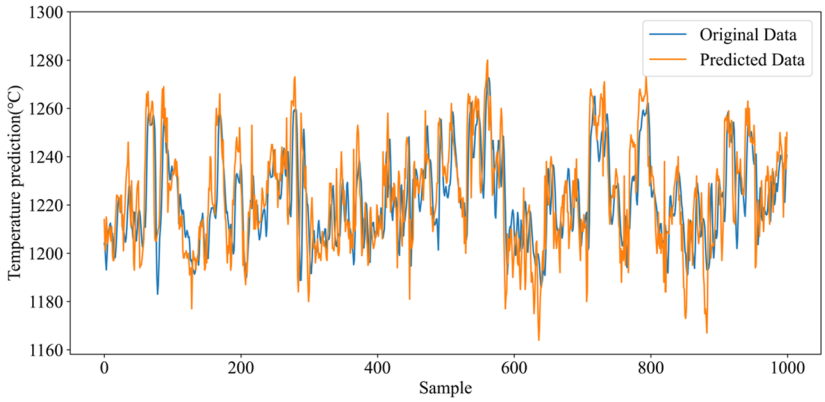

(b) Prediction result of GRU on univariate time series data

Figure 9. Prediction results of different algorithms on univariate time series data: (a) prediction results of Bi-GRU on univariate time series data and (b) prediction results of GRU on univariate time series data.

of pressure and temperature among the process variables are better than the flow rate because the flow rate varies over a larger range, which makes the problem of predicting the flow rate more challenging.

Results of the Effectiveness of Fusion Strategies. The comparisons are separately performed using univariate and multivariate time series data for fault diagnosis. There are also univariate and multivariate time series data together and two fusion methods for fault diagnosis. The two fusion approaches are representing univariate time series data by deep belief network (DBN), representing multivariate time series data by CNN and then finally fusing them by multilayer perceptron (MLP)[40] and representing multivariate time series data through CNN and then time series data through IFTD for time-frequency analysis[40] and finally fusing all the representations by MLP.

The results of the fusion comparison are shown in Table 6. The results show in Table 6 that our proposed method has the best indicators. The faults cannot be effectively recognized by relying on data from a single source. The other two fusion methods, which extract only the features of the temporal characteristics of the data, do not model the aspects of the correlation that exist between the process variables.

The experimental results show that our proposed method is superior to those of other fusion strategies. Univariate or multivariate time series data rely only on a single source of data for fault diagnosis; thus, they cannot give a comprehensive fault diagnosis result. Our approach is preferable because more information is obtained by fusing different data sources. The underperformance when using both univariate and multivariate time series data for fault diagnosis is that only temporal information on the data is considered without considering the correlation among the process variables of the furnace. From the experimental results, DBN + CNN has better performance than the univariate/multivariate time series representation. The possible reason is that they are good at learning temporal information. However, the performance of DBN + CNN is worse than that of our proposed algorithm, since they focused on only the local correlation of process variables, which leads to less ability to learn the global correlation of process variables. Moreover, the arrangement of variables in industrial data is typically based on the reaction orders of process equipment and work stages, thus the variables not only show correlations with their adjacent nodes but also have great relationships with ones that are far away in the topological structure.[40] In addition to the different representations of data, the DBN + CNN method and IFTD + ICNN method are also different in the fusion strategy. The DBN + CNN method and IFTD + ICNN method are represented by univariate time series data for DBN, multivariate time series data for CNN, univariate time series data for IFTD, and multivariate time series data for ICNN. The representation is later fused by MLP. Our proposed algorithm uses transformer to fuse data. The structure in the transformer is based on the self-attention mechanism, which allows the mode to handle the input sequence by considering information from all positions

https://doi.org/10.1021/acsomega.4c10552
ACS Omega 2025, 10, 13169−13184

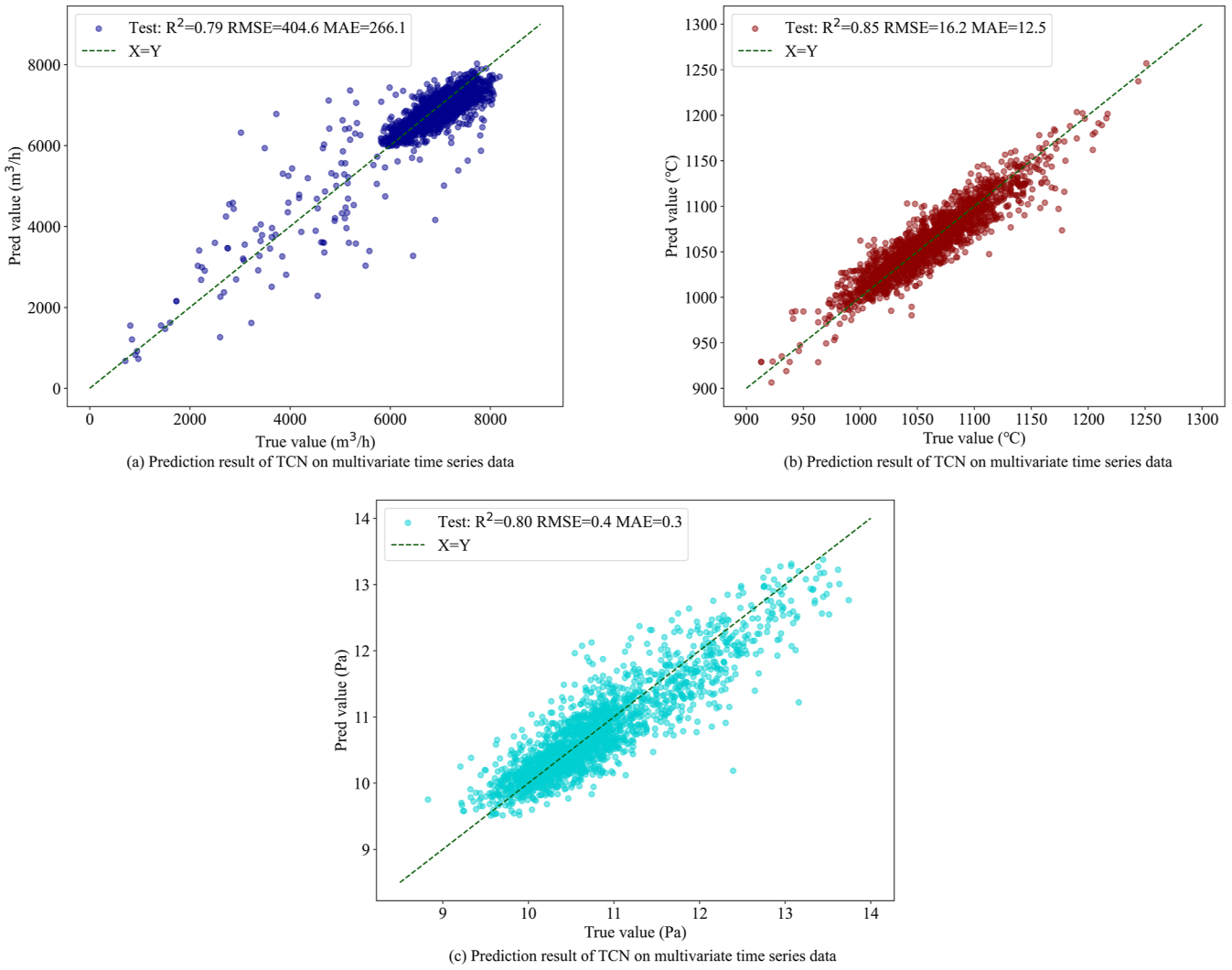

Figure 10. Prediction results for multivariate time series with different process variables.

Table 3. Prediction Results of Different Algorithms for Gas Flow at One Site in the Reheating Furnace

	TCN	LSTM	Seq2Seq	XGboost	ARIMA
RMSE	404.641	603.546	601.116	541.082	782.911
MAE	266.066	391.961	378.090	329.151	448.435
R^2	0.787	0.526	0.531	0.619	0.203

Table 4. Prediction Results of Different Algorithms for Furnace Temperature at One Site in the Reheating Furnace

	TCN	LSTM	Seq2Seq	XGboost	ARIMA
RMSE	16.223	17.840	30.992	20.431	37.592
MAE	12.514	13.850	24.370	15.224	29.595
R^2	0.854	0.824	0.469	0.769	0.219

Table 5. Prediction Results of Different Algorithms for Pressure at One Site in the Reheating Furnace

	TCN	LSTM	Seq2Seq	XGboost	ARIMA
RMSE	0.357	0.381	0.403	0.425	0.732
MAE	0.273	0.293	0.308	0.320	0.562
R^2	0.802	0.774	0.748	0.719	0.171

Table 6. Evaluation of Different Fusion Algorithms in Actual Production Data

method	accuracy (%)	precision (%)	recall (%)	F1-score
MSIF	91.33	91.46	92.59	92.02
univariate time series representation	57.5	67.72	72.81	70.17
multivariate time series representation	63.16	70.92	75.37	73.08
univariate + multivariate time series representation	69.83	78.12	75.56	76.81
DBN + CNN	88.16	89.02	89.82	89.41
IFTD + ICNN	78.50	80.00	84.74	82.30

simultaneously. This mechanism allows transformer to process the data at each time point while considering other time points in the sequence, thus easily capturing dependencies over long distances in the time series. Such a characteristic also makes our proposed method have a better effect on fusion than MLP or aggregation operations on fusing data from multiple sources into a single representation.

Result of Process Monitoring. In order to verify the validity of the proposed method, MSIF is compared with different methods to verify the effectiveness of the monitoring algorithm. In order to demonstrate the effectiveness of the

https://doi.org/10.1021/acsomega.4c10552
ACS Omega 2025, 10, 13169−13184

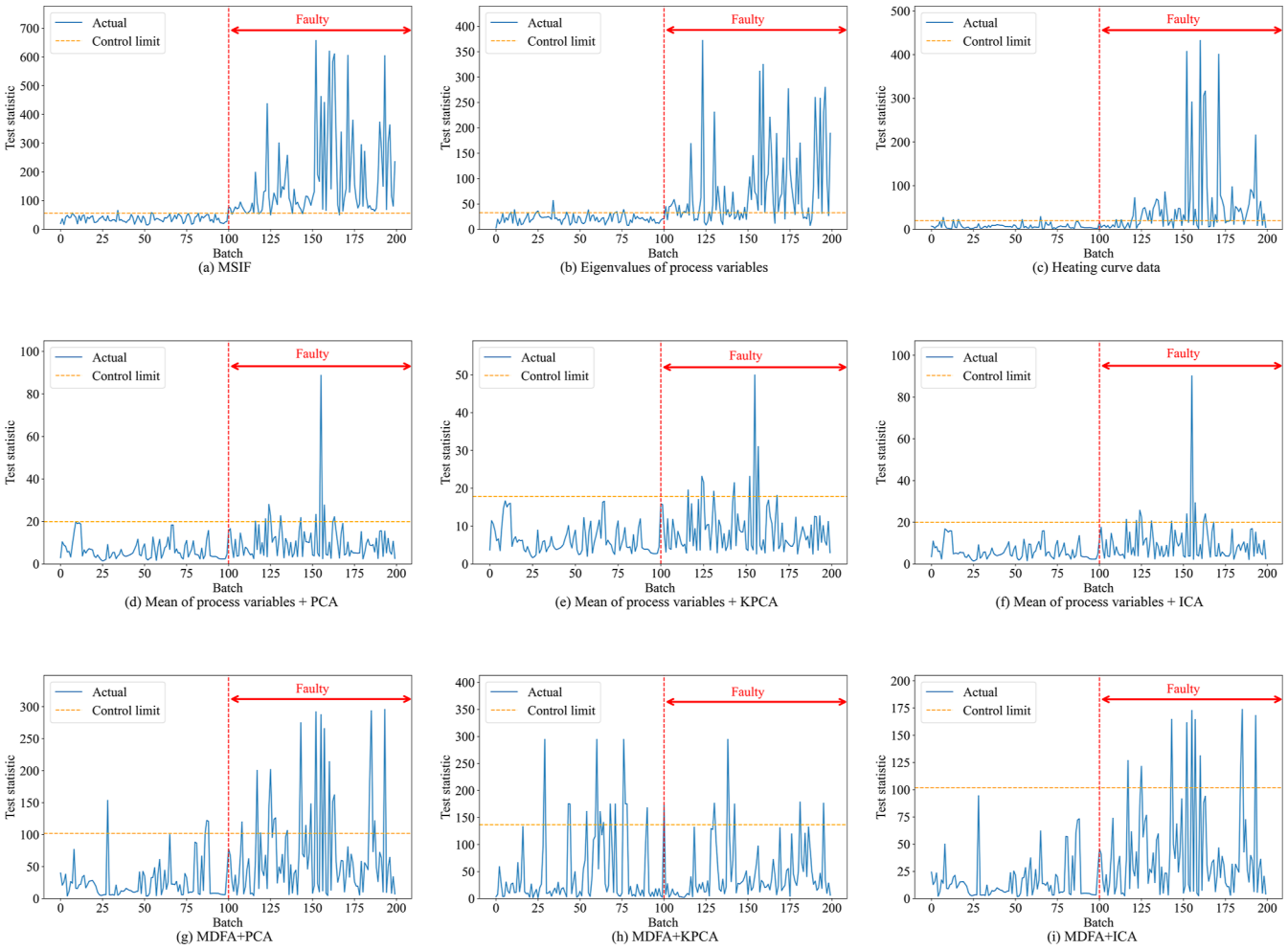

Figure 11. Predicting results of different algorithms in actual production data.

fusion scheme, a comparison is made with monitoring of a single object, specifically monitoring only the correlation of process data and monitoring only the heating curve data. The algorithm for the comparison also has the mean value of the process variable changing during the heating of the slab with PCA, KPCA, and ICA. The data preprocessing method MDFA[7] designed for reheating furnaces is combined with PCA, KPCA, and ICA.

The first 100 batches in Figure 11 are normal batches and the last 100 are faulty batches. The yellow line is the corresponding control limit, the one above the control limit is a faulty batch and the one below the control limit is a normal batch. The specific evaluation metrics are shown in Table 7. From the table, we can see that MSIF has the highest accuracy rate of 95%. In terms of the false alarm rate, two batches have incorrect results. However, the results calculated for these two batches are also very close to the control limits. From the results, it can be seen that the MSIF provides more accurate results than both monitoring the heating curve data of one batch and monitoring the process variables of the reheating furnace for one batch time. It can also be seen from the results that monitoring the process variables of the furnace does not give the desired results for abnormal batches. It is not possible to effectively distinguish the monitoring results of batches because of strong delay inside the reheating furnace. The reason for this delay is that it takes time to change the furnace temperature by controlling the gas valve. Another reason for the delay is that the length of the furnace is very long, and it usually requires quite a while to change the local temperature to achieve a uniform temperature field across the whole furnace. The results also show that there is not much difference between PCA and ICA and that using KPCA will partially improve the results. However, it is still not possible to monitor the abnormal batches effectively.

Table 7. Evaluation of Different Process Monitoring Algorithms in Actual Production Data

method	accuracy (%)	precision (%)	recall (%)	F1-score
MSIF	95	93.45	97.08	95.23
eigenvalues of process variables	78.5	76.33	89.28	82.29
heating curve	76	68.96	97.08	80.63
mean of process variables + PCA	54	52.35	99	68.48
mean of process variables + KPCA	54	52.08	100	0
mean of process variables + ICA	55	52.63	100	0
MDFA + PCA	59	55.86	97.08	70.91
MDFA + KPCA	50	53.19	89.28	66.67
MDFA + ICA	54.5	52.35	100	0

For the process variables, MDFA is more effective than just calculating the mean value. However, MDFA requires the

https://doi.org/10.1021/acsomega.4c10552
ACS Omega 2025, 10, 13169−13184

mean values, covariates between variables, higher-order statistics, etc. to be calculated. The process variables of a batch usually reach more than 1000 dimensions in this way. The dimensionality is then reduced through various dimensionality reduction algorithms, which may result in the loss of important information as well as weakening the algorithm's performance. In summary, MSIF for the reheating furnace gives satisfactory monitoring results.

CONCLUSIONS

In this paper, a novel process monitoring algorithm named MSIF for reheating furnaces was established. In order to obtain a more complete understanding of the production process and to accomplish more precise monitoring, two different parts of data are monitored, which are process variable data of the furnace that correspond to the heating time for each batch as well as the heating curve for every batch. In the part of process variable data, the correlation and temporal variation among process variables are monitored. The correlation is represented by eigenvalue decomposition, and temporal variation is represented by TCN. Heating curve data are temporal represented by Bi-GRU. All the obtained representations are fused by using transformer. The effectiveness of representation of univariate and multivariate time series data, fusion capability, and process monitoring performance are demonstrated on actual production data.

AUTHOR INFORMATION

Corresponding Author

Yang Yang − *Liaoning Engineering Laboratory of Data Analytics and Optimization for Smart Industry, Shenyang 110819, China;* orcid.org/0000-0003-4540-0908; Email: yangyang@ise.neu.edu.cn

Authors

Yunqi Ban − *National Frontiers Science Center for Industrial Intelligence and Systems Optimization, Northeastern University, Shenyang 110819, China; Key Laboratory of Data Analytics and Optimization for Smart Industry (Northeastern University), Ministry of Education, Shenyang 110819, China*

Yanyan Zhang − *National Frontiers Science Center for Industrial Intelligence and Systems Optimization, Northeastern University, Shenyang 110819, China*

Xianpeng Wang − *Key Laboratory of Data Analytics and Optimization for Smart Industry (Northeastern University), Ministry of Education, Shenyang 110819, China;* orcid.org/0000-0001-8132-9446

Zhenyu Wu − *Department of Industrial Engineering and Management, Shanghai Jiao Tong University, Shanghai 200240, China*

Complete contact information is available at: https://pubs.acs.org/10.1021/acsomega.4c10552

Notes

The authors declare no competing financial interest.

ACKNOWLEDGMENTS

This work was supported by the Major Program of National Natural Science Foundation of China [72192830, 72192831] and the 111 Project [B16009].

REFERENCES

(1) Wei, S.; Ye, C.; Zhao, Y.; Zhang, X.; Song, Z. M. D. F. F. MDFF: A Multilevel Deep Fusion Framework of Multisource Heterogeneous Data for FeO Content Prediction in Sintering Process. *IEEE Trans. Instrum. Meas.* **2025**, *74*, 1−11.

(2) Qian, J.; Deng, L.; Zhang, X.; Pi, S.; Song, Z.; Zhang, X. XAIP: An eXplainable aI-based pipeline for identifying key factors of surface defects in strip steel. *Steel Res. Int.* **2025**, *96*, 2400499.

(3) Yan, F.; Zhang, X.; Yang, C.; Hu, B.; Qian, W.; Song, Z. Data-driven modelling methods in sintering process: current research status and perspectives. *Can. J. Chem. Eng.* **2023**, *101*, 4506−4522.

(4) Zhang, C.; Dong, J.; Peng, K.; Zhang, H. Quality-related spatio-temporal information analytics-based multiunit synergetic monitoring for plant-wide industrial processes. *IEEE Trans. Autom. Sci. Eng.* **2024**, *22*, 1−13.

(5) Dong, J.; Tian, Y.-Z.; Peng, K.-X. Local multi-model integrated soft sensor based on just-in-time learning for mechanical properties of hot strip mill process. *J. Iron Steel Res. Int.* **2021**, *28*, 830−841.

(6) Emadi, A.; Saboonchi, A.; Taheri, M.; Hassanpour, S. Heating characteristics of billet in a walking hearth type reheating furnace. *Appl. Therm. Eng.* **2014**, *63*, 396−405.

(7) Dong, J.; Tian, Y.; Peng, K. Just-in-time learning-based soft sensor for mechanical properties of strip steel via multi-block weighted semisupervised models. *IEEE Access* **2020**, *8*, 123869−123881.

(8) Singh, V. K.; Talukdar, P. Comparisons of different heat transfer models of a walking beam type reheat furnace. *Int. Commun. Heat Mass Transfer* **2013**, *47*, 20−26.

(9) Yang, Y.; Shi, X.; Liu, X.; Li, H. A novel MDFA-MKECA method with application to industrial batch process monitoring. *IEEE/CAA J. Autom. Sin.* **2020**, *7*, 1446−1454.

(10) Tang, L.; Meng, Y. Data analytics and optimization for smart industry. *Front. Eng. Manage.* **2021**, *8*, 157.

(11) Lu, B.; Chen, D.; Chen, G.; Yu, W. An energy apportionment model for a reheating furnace in a hot rolling mill − A case study. *Appl. Therm. Eng.* **2017**, *112*, 174−183.

(12) Yang, Y.; Shi, X.; Yi, S.; Chen, X.; Qin, S. A novel process monitoring method based on improved DTW-MKECA. *29th Chinese Control And Decision Conference (CCDC)*, 2017.

(13) Zhou, B.; Ye, H.; Zhang, H.; Li, M. Process monitoring of iron-making process in a blast furnace with PCA-based methods. *Control Eng. Pract.* **2016**, *47*, 1−14.

(14) Cao, Y.; Yuan, X.; Wang, Y.; Gui, W. Hierarchical hybrid distributed PCA for plant-wide monitoring of chemical processes. *Control Eng. Pract.* **2021**, *111*, 104784.

(15) Dong, Y.; Qin, S. J. A novel dynamic PCA algorithm for dynamic data modeling and process monitoring. *J. Process Control* **2018**, *67*, 1−11. Big Data: Data Science for Process Control and Operations

(16) Kim, D.; Lee, I.-B. Process monitoring based on probabilistic PCA. *Chemom. Intell. Lab. Syst.* **2003**, *67*, 109−123.

(17) Huang, J.; Yan, X. Quality-driven principal component analysis combined With kernel least squares for multivariate statistical process monitoring. *IEEE Trans. Control Syst. Technol.* **2019**, *27*, 2688−2695.

(18) Wang, Y.; Sun, F.; Li, B. Multiscale neighborhood normalization-based multiple dynamic PCA monitoring method for batch processes with frequent operations. *IEEE Trans. Autom. Sci. Eng.* **2018**, *15*, 1053−1064.

(19) Li, H.; Jia, M.; Mao, Z. Time-slice dynamic prediction and multiway serial PCA for batch industrial process monitoring. *Comput. Chem. Eng.* **2024**, *182*, 108580.

(20) Cheng, C.-Y.; Hsu, C.-C.; Chen, M.-C. Adaptive kernel principal component analysis (KPCA) for monitoring small disturbances of nonlinear processes. *Ind. Eng. Chem. Res.* **2010**, *49*, 2254−2262.

(21) Cho, J.-H.; Lee, J.-M.; Wook Choi, S.; Lee, D.; Lee, I.-B. Fault identification for process monitoring using kernel principal component analysis. *Chem. Eng. Sci.* **2005**, *60*, 279−288.

(22) Jiang, Q.; Yan, X. Parallel PCA−KPCA for nonlinear process monitoring. *Control Eng. Pract.* **2018**, *80*, 17−25.
(23) Fezai, R.; Mansouri, M.; Taouali, O.; Harkat, M. F.; Bouguila, N. Online reduced kernel principal component analysis for process monitoring. *J. Process Control* **2018**, *61*, 1−11.
(24) Deng, X.; Tian, X.; Chen, S.; Harris, C. J. Nonlinear process fault diagnosis based on serial principal component analysis. *IEEE Trans. Neural Networks Learn. Syst.* **2018**, *29*, 560−572.
(25) Kano, M.; Hasebe, S.; Hashimoto, I.; Ohno, H. A new multivariate statistical process monitoring method using principal component analysis. *Comput. Chem. Eng.* **2001**, *25*, 1103−1113.
(26) Yao, Y.; Gao, F. Batch process monitoring in score space of two-dimensional dynamic principal component analysis (PCA). *Ind. Eng. Chem. Res.* **2007**, *46*, 8033−8043.
(27) Guo, R.; Zhang, N. A process monitoring scheme for uneven-duration batch process based on sequential moving principal component analysis. *IEEE Trans. Control Syst. Technol.* **2020**, *28*, 583−592.
(28) Hsu, C.-C.; Chen, M.-C.; Chen, L.-S. Integrating independent component analysis and support vector machine for multivariate process monitoring. *Comput. Ind. Eng.* **2010**, *59*, 145−156.
(29) Hsu, C. C.; Chen, L. S.; Liu, C. H. A process monitoring scheme based on independent component analysis and adjusted outliers. *Int. J. Prod. Res.* **2010**, *48*, 1727−1743.
(30) Jiang, Q.; Yan, X. Non-Gaussian chemical process monitoring with adaptively weighted independent component analysis and its applications. *J. Process Control* **2013**, *23*, 1320−1331.
(31) Zhu, J.; Ge, Z.; Song, Z. Non-gaussian industrial process monitoring with probabilistic independent component analysis. *IEEE Trans. Autom. Sci. Eng.* **2017**, *14*, 1309−1319.
(32) Zhou, P.; Zhang, R.; Xie, J.; Liu, J.; Wang, H.; Chai, T. Data-driven monitoring and diagnosing of abnormal furnace conditions in blast furnace ironmaking: an integrated PCA-ICA method. *IEEE Trans. Ind. Electron.* **2021**, *68*, 622−631.
(33) Xu, Y.; Shen, S.-Q.; He, Y.-L.; Zhu, Q.-X. A novel hybrid method integrating ICA-PCA with relevant vector machine for multivariate process monitoring. *IEEE Trans. Control Syst. Technol.* **2019**, *27*, 1780−1787.
(34) Xue, Y.; Wen, C.; Wang, Z.; Liu, W.; Chen, G. A novel framework for motor bearing fault diagnosis based on multi-transformation domain and multi-source data. *Knowl. Based Syst.* **2024**, *283*, 111205.
(35) Han, D.; Zhang, Y.; Yu, Y.; Tian, J.; Shi, P. Multi-source heterogeneous information fusion fault diagnosis method based on deep neural networks under limited datasets. *Appl. Soft Comput.* **2024**, *154*, 111371.
(36) Wang, X.; Yan, J. Deep learning based multi-source heterogeneous information fusion framework for online monitoring of surface quality in milling process. *Eng. Appl. Artif. Intell.* **2024**, *133*, 108043.
(37) Son, Y.-H.; Shin, D.-H.; Kam, T.-E. FTMMR: Fusion Transformer for Integrating Multiple Molecular Representations. *IEEE J. Biomed. Health Inf.* **2024**, *28*, 4361−4372.
(38) Hochreiter, S.; Schmidhuber, J. Long short-term memory. *Neural Comput.* **1997**, *9*, 1735−1780.
(39) Lea, C.; Flynn, M. D.; Vidal, R.; Reiter, A.; Hager, G. D. Temporal convolutional networks for action segmentation and detection. *2017 IEEE Conference on Computer Vision and Pattern Recognition (CVPR)*, 2017; pp 1003−1012.
(40) Yuan, X.; Wang, Y.; Wang, C.; Ye, L.; Wang, K.; Wang, Y.; Yang, C.; Gui, W.; Shen, F. Variable correlation analysis-based convolutional neural network for far topological feature extraction and industrial predictive modeling. *IEEE Trans. Instrum. Meas.* **2024**, *73*, 1−10.

https://doi.org/10.1021/acsomega.4c10552
ACS Omega 2025, 10, 13169−13184